

COMPACT HIGH FIELD IGNITION TEST REACTORS
USING COMPRESSION-BOOSTED NEUTRAL BEAM HEATING

L. Bromberg, D.R. Cohn and J.E.C. Williams

April 1978
MIT Plasma Fusion Center Report RR-78-4

**Compact High Field Ignition Test Reactors
Using Compression-Boosted Neutral Beam Heating^x**

by

L. Bromberg, D. R. Cohn and J. E. C. Williams

Francis Bitter National Magnet Laboratory[†]

and

Plasma Fusion Center[‡]

Massachusetts Institute of Technology

Cambridge, Ma 02139

MIT Plasma Fusion Center Report RR-78-4

^xWork supported by U.S. Department of Energy Contract # ET-78-S-02-4646

[†]Supported by National Science Foundation.

[‡]Supported by U. S. Department of Energy.

Abstract

A parametric study has been used to develop a preliminary design of a compact ignition reactor. A key feature of the design is the use of copper *TF* plates of Bitter construction in order to accommodate the relatively high stresses (~ 50 kpsi) required for a compact device. The purpose of the high field ignition test reactor *HFITR* is to study alpha particle heating and the burn dynamics of ignited plasmas. Adiabatic compression in major radius of a neutral beam heated tokamak plasma reduces the beam voltage required for adequate penetration permitting the use of 120 keV D^0 beams. It may also be possible to use adiabatic adjustment of major radius to control thermal runaway after ignition has been achieved. The parametric study indicates that the magnet and neutral beam requirements do not appear to depend strongly upon magnetic field for magnetic fields at the compressed plasma in the range 10 - 15 T. A preliminary design has been developed for a device with a magnetic field on axis of the compressed plasma of 12.5 T. The major radius of the center of the magnet bore is 1.95 m and the magnetic field at the center of the magnet bore is 8.1 T. The major radius of the compressed plasma is 1.3 m and the minor radius is 0.35 m. The compression ratio is 2. A circular plasma is ignited with $\langle\beta\rangle \sim 3\%$. The machine requires 13 MW neutral beam power if the empirical scaling law is valid at the high temperatures. 6 beam ports, each with 0.2 m^2 , provide enough access for the neutral beams. The fusion power produced at ignition is 80 MW. A 200 MW power supply is enough to drive the *TF* coil and the auxiliary systems, resulting in a toroidal magnetic field flat-top of 20 s. Compression requires pulsing 20 MJ in the equilibrium field system. The energy required for compression is provided by inductive storage coils charged by the *TF* power supply. The *OH* requirements are reduced by the generation of Volt-s by the vertical field.

I. Introduction

By utilizing high field copper magnet technology, preliminary design features have been derived for a compact (major radius at the center of the *TF* magnet = 1.95 m) ignition test reactor which utilizes neutral beam heating in conjunction with adiabatic compression. The purpose of this device is to study alpha heating and the burn dynamics of ignited plasmas. The fusion power produced under ignition conditions is only 80 MW. Approximately 13 MW of auxiliary heating is required to achieve the temperatures needed for ignition, where the plasma heating by energetic alpha particles alone (along with a negligibly small amount of ohmic heating) sustains the plasma temperature against thermal conduction and radiation losses.

Since the most effective auxiliary heating of present tokamaks plasmas has been achieved with neutral beams, this technique is used in the design presented here. "Compression-boosting" which involves adiabatic compression in major radius is used to reduce the beam voltage required for adequate penetration. A compression ratio of 2 permits the use of 120 keV D^0 beams. Although compression is used, the size of the present high field ignition test reactor *HFITR* is still modest. The major radius of the center of the toroidal field magnet bore is 1.95 m. The magnetic field at this position is 8.1 T. The major radius of the compressed plasma is 1.3 m, and the minor radius is 0.35 m. The toroidal field on the axis of the compressed plasma is 12.5 T. A parametric study has shown that the magnet and neutral beam requirements are not strongly dependent upon magnetic field in the range 10 - 15 T at the axis of the compressed plasma.

II. Plasma Parameters

The minimum plasma size in an ignited reactor is determined by the requirements of

sufficient plasma current to contain the alpha particles and by the requirement of $n\tau_e$. McAlees [1] has shown that the alpha containment depends mainly on the parameter $I_p A$, where I_p is the plasma current and A is the aspect ratio. The minimum minor radius is then given by

$$a > \frac{\mu_0}{2\pi} \frac{q_a}{B_T} (I_p A) \quad (1)$$

where q_a is the safety factor and B_T is the toroidal magnetic field on the axis.

According to the empirical scaling law [2,3],

$$(n_o \tau_e)_{emp} = 3.8 \cdot 10^{-19} (n_o a)^2 \text{ cm}^{-3} \text{ s} \quad (2)$$

where n_o is the electron density in cm^{-3} at the center of the machine and a is in cm. (The $q_a^{1/2}$ dependence of the scaling law [2,3] has been suppressed in view of recent experiments in *ALCATOR* [4] and *PULSATOR* [5]). We define a "margin of ignition" as

$$MI = \frac{(n_o \tau_e)_{emp}}{(n_o \tau_e)_{ign}} \quad (3)$$

where $(n_o \tau_e)_{ign}$ is the value of $(n_o \tau_e)$ required for ignition at a given temperature and $Z_{eff} = 1$. If the empirical scaling law holds at reactor temperatures and $Z_{eff} \approx 1$, then ignition is obtained with $MI = 1$.

For a plasma characterized by parabolic temperature and density profiles, the required value of $(n_o \tau_e)_{ign}$ is shown in Figure 1 as a function of the central temperature and the alpha containment parameter $I_p A$. Because of the high density operation, the ion and the electron temperatures are equal. At a central temperature of 15 keV, ignition occurs when $n_o \tau_e \approx 4.6 \cdot 10^{14} \text{ cm}^{-3} \text{ s}$ for $I_p A = 1.0 \cdot 10^7 \text{ A}$.

In order to reduce the neutral beam energy required for penetration, adiabatic

compression in major radius [6] is used to increase the plasma density after heating of the initial plasma with neutral beams. According to the empirical scaling law for the energy confinement, the value of $n_o \tau_e$ for the final plasma is related to the value of $n_o \tau_e$ of the initial plasma by

$$(n_o \tau_e)_f = C^3 (n_o \tau_e)_i \quad (4)$$

where C is the compression ratio [7]. The plasma temperature is related to the initial temperature by

$$T_f = C^{4/3} T_i \quad (5)$$

In order to obtain peaked energy deposition profiles with neutral beams injected in the near perpendicular direction, it is necessary that [8]

$$W_b \approx 9.0 \cdot 10^{-15} n_o a \text{ keV} \quad (6)$$

where W_b is the D^0 beam energy, n_o is in cm^{-3} and a in cm. Combining (2) and (6), we find that the beam energy required for heating to ignition goes as

$$W_b = 1.5 \cdot 10^{-5} [M I (n_o \tau_e)_{\text{emp}}]^{1/2} \text{ keV} \quad (7a)$$

Fig. 2 from [7] shows how W_b decreases with increasing temperature. $I_p A = 3.7 \cdot 10^6 \text{ A}$, and $\sim 80\%$ of the fast alpha particles are confined. Beam energies greater than 200 KeV are required. If compression is used to arrive to the final state, then the beam energy requirement is reduced to [7]

$$W_b \approx 1.5 \cdot 10^{-5} [M I (n_o \tau_e)_{\text{emp}}]^{1/2} \frac{1}{C^{3/2}} \text{ keV} \quad (7b)$$

where C is the compression used. Even moderate compression ratios reduce the beam energy significantly, as shown in Figure 2. However, the required beam power increases

with compression. The beam power is shown in Figure 3 for different final plasma temperatures as a function of the compression ratio for a plasma with a final major radius of 1.3 m and $I_p A = 8.7 \cdot 10^6$ A. The power increase results from the decrease in alpha particle heating that accompanies the decrease in the initial plasma density and temperature.

Two margins of ignition can be defined. One is determined by the constraint on n_o , and thus on $n_o \tau_e$, imposed by a limit on the toroidal beta:

$$MI_{\text{beta}} = \frac{(n_o \tau_e)_{\text{max beta}}}{(n_o \tau_e)_{\text{ign}}} \sim \beta_{\text{crit}}^2 \frac{B_T^4 a^2}{A^2} \sim \frac{B_T^4 a^2}{A^2} \quad (8)$$

for constant plasma temperature. Here $(n_o \tau_e)_{\text{max beta}}$ is the value of the confinement quality parameter (2) evaluated at the beta limit, assumed to be given by [9,10]

$$\beta_{\text{crit}} = \frac{1}{A q_a^2} \quad (9)$$

The other margin of ignition is determined by the constraint on n_o imposed by beam penetration requirements

$$MI_{\text{beam}} = \frac{(n_o \tau_e)_{\text{beam}}}{(n_o \tau_e)_{\text{ign}}} \sim W_b^2 C^3 \quad (10)$$

where $(n_o \tau_e)_{\text{beam}}$ is the value of the confinement quality parameter determined by beam penetration limits [7].

Figure 4 shows the margins of ignition as functions of the toroidal magnetic field on the axis of the compressed plasma for a 3.05 m wide Bitter plate and $\sigma_{TF} = 3.6 \cdot 10^8$ Pa (50 Kpsi), where σ_{TF} represents the vertical stresses in the inboard region of the TF magnet. These stresses are the largest stresses in this magnet. 0.15 m is allowed between the plasma and the TF coil for a limiter, the vacuum wall bellows, etc. Figure 4

is drawn for $q_a = 2.5$ and $I_p A = 8.7 \cdot 10^6$ A. For these conditions, $\sim 80\%$ of the alphas are born on confined orbits [1]. MI_{beam} has a flat maximum for a magnetic field of ~ 12.5 T. MI_{beta} decreases with increasing magnetic field larger than 10 T as a result of the increased aspect ratio created by an increase in the thickness of the TF magnet. R , the major radius of the compressed plasma, is relatively constant at these fields, as can be seen in Figure 4 because $MI_{beta} \sim B_T^4 a^2 / A^2 \sim 1/R^2 (I_p A)^4$. MI_{beam} decreases with field because the compression ratio is reduced due to an increase in the minor radius. As the magnetic field of the compressed plasma decreases below 8 T the bending stresses in the magnet increase as a consequence of the magnet becoming thinner. Furthermore, since A decreases, $I_p \sim 1/A$ increases and larger OH and EF drives are required. As a result of these additional factors, the performance of a device with fixed stresses and plate size begins to fall off sharply for fields less than 8 T.

Figure 5 shows the maximum values of MI_{beam} and MI_{beta} as a function of the stresses in the trunk section of the TF bore. This figure is drawn for $I_p A = 8.7 \cdot 10^6$ A and for $q_a = 2.5$. r_{ohm} , the size of the OH bore, is 0.35 m in Figures (4) and (5). (Both MI_{beta} and MI_{beam} are only weakly dependent on r_{ohm} , which is mainly determined by the stresses in the OH transformer calculated in the next section). The maximum stresses in the inboard section of the TF coil, σ_{TF} , have been set to $3.6 \cdot 10^8$ Pa. This value corresponds to the stresses in ALCATOR C [11] and are close to the maximum allowable stresses when Bitter-type copper plates are reinforced using stainless steel.

Figure 6 shows the maximum margin of ignition MI_{beam} and the corresponding value of MI_{beta} as a function of the alpha containment parameter $I_p A$ for $q = 2.5$, $r_{ohm} = 0.35$ m and $\sigma_{TF} = 3.6 \cdot 10^8$ Pa. The plate size is 3.05 m. MI_{beta} increases with increasing $I_p A$. MI_{beam} , on the other hand, decreases with increasing $I_p A$, as a result of the smaller compression ratios due to larger minor plasma radii.

Figure 7 shows the outer radius of the TF coil, R_{out} , as a function of $I_p A$, for $MI_{beam} = 1$. For a given value of $I_p A$, the machine size R_{out} is varied until the optimized value of the margin of ignition is unity, $MI_{beam} = 1$. The other dimensions are the same as Figure 4. Also shown is the corresponding value of MI_{beta} . There is a compromise between small machine size, R_{out} and large value of $I_p A$, which determines the alpha containment properties. If necessary, improved alpha containment can be achieved by increasing slightly the outer radius of the TF coil, as shown in Figure 7. Another method of improving the alpha confinement is by running at lower values of q_a .

In order to allow for temperature excursions of the ignited plasma of $\Delta T/T \approx 50\%$, $MI_{beta} \approx 2$. If $MI \approx 2$ must be used to achieve ignition because of impurities or degradation in τ_e , then only a small thermal excursion would be tolerated. According to Figure 7, $MI \approx 2$ when

$$I_p A = 8.7 \cdot 10^8 \text{ A} \quad (10)$$

For this value of $(I_p A)$ McAless [1] has determined that $\approx 80\%$ of the alpha particles are born in contained orbits. It should be stressed the fact that McAlees [1] has calculated the lost fractions assuming flat current profiles. As the current distribution is probably peaked in the center, this is a pessimistic assumption.

It is thought that good confinement of the alpha particles is necessary not only because it decreases the ignition requirements on the plasma (as shown in Figure 1), but because the unconfined fast alpha particles may sputter the wall and introduce impurities in the plasma. How much sputtering can be tolerated is not known, and the HFTR design is a tradeoff between large $I_p A$ (that is, good confinement of the alpha particles), and small dimensions.

Compression-boosted machines have a built-in method of controlling the thermal

runaway by adiabatically adjusting the major radius. Some temperature excursion is allowed in the design. Furthermore, the introduction of cold gas around the compressed plasma can reduce the wall sputtering and reduce the impurity influx.

Table I shows the design parameters. The burn time, if limited by heating of the *TF* coils, can be $\sim 40 \tau_e$, but would require a total energy of ~ 2000 GJ.

In order to see what happens as the energy confinement time (2) degrades with temperature, a multiplier Q is defined as

$$Q = \frac{P_{\text{plasma, comp}}}{P_{\text{beam, uncomp}}} \quad (11)$$

where $P_{\text{plasma, comp}}$ is the total (alpha plus neutron) power from the compressed plasma and $P_{\text{beam, uncomp}}$ is the beam power required to bring the plasma to the precompressed temperature. Figure 8 shows Q vs the degradation of the energy confinement time. The same degradation is assumed in the precompressed and compressed states. Note that Q is finite (because of the definition) at ignition, which occurs when no degradation of the energy confinement time occurs.

III. Magnetic field system

An elevation view of the magnet system is shown in Figure 9. The major radius of the center of the *TF* magnet bore is 1.3 m.

Adiabatic compression of a plasma by reducing the major radius was the technique used on the *ATC* machine [12, 13], where a rapid increase in the vertical magnetic field provided the driving force. For the *HFTR*, however, increasing a vertical field with small radial gradients results in large peak power requirements: for the compression to occur in a time scale short compared with the energy confinement time (~ 0.2 s) a peak power

of ≈ 1000 MW would be needed.

A slight variation of this method is to create a vertical field with a significant radial gradient, such that as the plasma moves to smaller major radii, the static magnetic field increases. The power required to increase the vertical field can be reduced. In fact, it has been calculated [14] and tested experimentally [13] that if the magnetic field varies as

$$\frac{R}{B_{\text{vert}}} \frac{dB_{\text{vert}}}{dR} < -\frac{3}{2}$$

then the plasma self-compresses. This selfcompression occurs without the need of increased ohmic drive and generates a plasma skin current. Very fast compression times can be achieved this way. In spite of the field gradient, the plasma shape is close to circular [15].

In order to avoid the problem of skin current generation, self-compression is not used. However, some gradient is used to reduce the *EF* drive requirements:

$$\frac{R}{B_{\text{vert}}} \frac{dB_{\text{vert}}}{dR} \approx -1.3$$

Preliminary coil positions are listed in Table II, together with the corresponding currents. Three sets of coils are enough. This set of coils required an energy swing of 20 MJ for compression, as compared with ~ 80 MJ for a field with a smaller gradient. The power required to achieve compression is therefore significantly reduced by properly shaping the vertical field. The large gradient of B_{vert} also helps provide extra Volt-s to establish the plasma current, and therefore reducing the requirements of the *OH* transformer.

The *TF* coils are made out of copper plates reinforced by stainless steel plates. In this way, stresses of the order of $3.6 \cdot 10^8$ Pa in the inboard of the *TF* coil can be tolerated [11]. The height of the plates is chosen so that the bending stresses of the

TF coil are within the elastic limit for copper. The bending stresses are $\sim 2.2 \cdot 10^8$ Pa if the width of the plates is 2.5 m. This is consistent with the positions of the *EF* coils. The pulse length is determined by the maximum power available, subject to constrain that the maximum temperature rise in the *TF* coil be less than ~ 200 °K. The *TF* magnet is "inertially cooled", that is, no cooling during the pulse. If the maximum power available to drive the *TF* is 200 MW, the flat top is ~ 20 s long. Approximately 8000 l of liquid nitrogen are evaporated in order to cool the magnet after a 20 s ignited pulse. The parameters of the *TF* magnet are shown in Table III.

The stresses on the *OH* coil are determined by the flux swing required by the plasma to establish the current and the size of the *OH* coil bore, r_{ohm} . The fluxes produced by the *EF*, and *OH* at both the initial plasma location and at the final plasma position are listed in Table IV. It is interesting to note that compression does not required much change of the *OH* flux.

The flux needed can be produced with stresses in the *OH* coil less than $6.5 \cdot 10^7$ Pa if $r_{ohm} \approx 0.35$ m.

The absence of neutron shielding between the plasma and the *TF* coils places stringent requirements on the insulation between copper turns. The compression stresses in the insulator due to the inward forces in the *TF* magnet are $7 \cdot 10^7$ Pa. This precludes the use of glass bonded mica which would be crashed by the compressive stresses. Because of the large vertical forces in the trunk of the *TF* magnet, the stainless steel-copper composite will be strained by $\sim 0.3\%$, resulting in stresses beyond the tensile stress of ceramics.

The one dimensional neutron transport code *AN/ISN* has been used to determine the neutron flux in the *TF* region. The inferred life expentancies of organic and inorganic

insulators are shown in Table V. It is possible to increase the life expectancy of the insulators by providing some shielding. This can be done without having to increase the *TF* coil bore by receding the insulation away from the plasma, as shown in Figure 10. The compressive stresses are increased by this method because the contact area between adjacent plates has been reduced. This self-shield can be ~ 0.15 m thick without perturbing the *TF* magnet. The neutron flux at the insulator is not decreased significantly but the energy spectra is softened substantially. Furthermore, a two dimensional transport code is being used to take into account the toroidal geometry. It is expected that this will decrease the neutron fluence on the insulator on the inboard region of the *TF* coil.

The possibility of using anodized aluminum plates with or without synergistic coatings [16] is being considered; tests are being performed to evaluate its behavior under large strain and neutron fluences.

Due to the large heat loading of the first wall (~ 80 w/cm²), it is necessary to cool it during the pulse. The problems of cooling are being studied; the beam ports have been overdesigned to allow cooling access. If the first wall is not dynamically cooled, the pulse length would be limited to 3 - 10 s, depending on the thickness of the first wall. Approximately 16 MW must be removed from the first wall during the ignited phase of the pulse.

IV. Neutral Beams System and Port Design

As shown in Figure 3, the compression technique reduces the beam energy required while increasing the beam power. However, because the initial plasma position is at a larger major radius, there is more access for the beams. Near perpendicular injection of 12.5 MW of 120 keV is used. This method is being used in *TFR* [17].

Assuming that the power density per unit area is $\sim 2 \text{ kW/cm}^2$ [18], then in order to inject $\sim 12 \text{ MW}$ of beams, 0.6 m^2 of neutral-beam access is necessary. Six ports, each with 0.2 m^2 are more than sufficient. To prevent the escape of fast injected ions, the magnetic field ripple must be kept small; special coils are provided to reduce the ripple. The plasma current of the initial plasma is 1.2 MA and $A \approx 5$. This should provide good confinement of the injected 120 keV ions [8].

The port design is shown in Figure 11, which also shows the ripple cancelling coils. The field ripple is shown in Figure 12. The ripple decreases to very low levels at the position of the compressed plasma.

In order to prevent ripple trapping of the fast neutrals, the ripple must be [19]

$$\delta_o < \frac{2r}{R} \frac{|\sin(\theta)|}{N q_a} \quad (12)$$

where θ is the poloidal angle and N is the number of ports. Figure 12 shown that this criteria is satisfied almost everywhere in the plasma.

The ripple cancelling coils require a substantial current. In this preliminary design, each ripple cancelling coil carries $\sim 2 \text{ MA}$. Although this current is large for coils of this size, the coils will have to be energized only during a short period of the pulse, when the plasma is in the precompressed state. The size of the ripple is $< 0.5\%$ at the position of the compressed plasma even when the ripple cancelling coils are turned off. It is also possible to reduce the size of the port by increasing the required neutral beam power density.

The beam port has been overdesigned to allow penetration of cooling lines. Although the toroidal field coils are "inertially cooled", the first wall needs to be cooled if

the pulse length is longer than ~ 3 s.

The beam energy, power requirements and port dimensions are shown in Table VI. The ripple cancelling coil parameters are given in Table VII.

VI. Conclusion

A parametric study has been used to develop a design for a small copper magnet (major radius of the center of the magnet bore = 1.9 m) ignition test reactor which is heated to ignition with 12.5 MW of 120 keV beams if the empirical scaling law is satisfied at high temperatures. A margin for temperature excursions is allowed for in the design. Adiabatic adjustment of major radius may provide a built-in temperature control that can be used to prevent thermal runaway at ignition.

Although $MI_{beam} \approx 1$, it is possible to increase this margin of ignition by either going to higher beam energy, by relaxing somewhat the beam deposition profile requirement (5) or by running at lower q_a (and therefore improving the alpha containment). It is reasonable to expect that $MI_{beam} = MI_{beta} = 2$ could be obtained. Thus some margin of safety against a degradation of the energy confinement time or the presence of impurities is possible.

The absence of neutron shielding reduces the size of the machine while limiting the life of the magnet. If appropriate inorganic insulation for the plates can be found, the machine life can be longer than 500000 burn-seconds. Otherwise, if reinforced organic insulators are used, the lifetime is reduced to ~ 5000 burn-seconds.

References

- [1] D. G. McAlees, Oak Ridge National Laboratory Report ORNL-TM-4661 (1974)
- [2] D. R. Cohn, R. R. Parker and D. L. Jassby, Nucl Fusion 16 31 (1976)
- [3] D. L. Jassby, D. R. Cohn and R. R. Parker, Nucl Fusion 16 1045 (1976)
- [4] D. Overskei, private communication
- [5] Pulsator group, private communication
- [6] H. P. Furth and S. Yoshikawa, Phys. Fluids 13 2593 (1970)
- [7] D. R. Cohn, D. L. Jassby and K. Kreischer, Princeton Plasma Physics Laboratory Report MATT-1405 (1978)
- [8] D. L. Jassby, Nucl Fusion 17 309 (1977)
- [9] A. M. M. Todd et. al, Phys. Rev. Lett. 38 826 (1977)
- [10] P. H. Rutherford et. al, Princeton Plasma Physics Laboratory Report MATT-1418 (1978)
- [11] C. Weggel et. al, in *Proceedings of the 7th Symposium on Engineering Problems of Fusion Research*, Knoxville, Tn, October 1977
- [12] U. R. Christensen et. al, Princeton Plasma Physics Laboratory Report MATT-847 (1971)
- [13] K. Bol et. al, Phys. Rev. Lett. 29 1495 (1972)
- [14] S. Yoshikawa, Phys. Fluids 7 278 (1964)
- [15] L. E. Zakharov, Sov. Phys.-Tech. Phys. 16 4 (1971)
- [16] C. P. Corvino, General Magnaplate Corp., private communication
- [17] TFR group, in *Plasma Physics and Controlled Nuclear Fusion Research* (Proc. 6th Int. Conf, Berchtesgaden, 1976) 1 IAEA, Vienna (1977)
- [18] H. Haselton, private communication
- [19] O. A. Anderson and H. P. Furth, Nucl Fusion 12 207 (1972)

List of Figures

- Figure 1. $(n_0 \tau_e)$ vs. T for different values of $I_p A$.
- Figure 2. Beam energy vs compression for different values of temperature.
- Figure 3. Beam power vs compression for different values of the temperature.
- Figure 4. MI_{beam} and MI_{beta} vs magnetic field on axis for a stress $\sigma_{TF} = 3.6 \cdot 10^8$ Pa. Bitter plate size is 3.0 m, $r_{ohm} = 0.35$ m. $q = 2.5$, $W_b = 120$ keV.
- Figure 5. MI_{beam} and MI_{beta} as a function of the stresses in the inboard section of the TF coil, σ_{TF} . Dimension are same as for Figure 4.
- Figure 6. MI_{beam} and MI_{beta} vs the parameter $I_p A$ for $q = 2.5$, $r_{ohm} = 0.35$, $W_b = 120$ keV and $\sigma_{TF} = 3.6 \cdot 10^8$ Pa. The Bitter plate is 3.05 m.
- Figure 7. MI_{beta} and R_{out} , the outer edge of the TF coil, vs $I_p A$ for $MI_{beam} = 1$.
- Figure 8. Q vs degrading of energy confinement time. $R_f = 1.28$ m, $a = 0.35$ m, $I_p A = 8.7 \cdot 10^6$ A, $T = 15$ keV. Same degradation of the energy confinement time at the precompressed and compressed states.
- Figure 9. Elevation view of the TF, OH and the EF coils.
- Figure 10. Increased shielding of the insulator in the inboard region of the TF coil.
- Figure 11. Port design.
- Figure 12. Magnetic field ripple induced by the beam ports.

List of Tables

Table I. Plasma Parameters after Compression

Table II. *EF* System Parameters

Table III. *TF* Magnet

Table IV. *OH* Magnet

Table V. Lifetime Expectancy of the Insulation

Table VI. Neutral Beam System

Table VII. Ripple Cancelling Coils

Table I

Plasma Parameters after Compression

C	2.0
R_F (m)	1.28
a_F (m)	0.35
B_T (T)	12.5
q_a	2.5
I (A)	2.5×10^6
n_c (cm^{-3})	1.0×10^{15}
T (keV)	15
$(n\tau_e)_{\text{emp}} / (n\tau_e)_{\text{ign}}$	1.0
$(n\tau_e)_{\text{max beta}} / (n\tau_e)_{\text{ign}}$	2.0
Plasma shape	circular
$\langle\beta\rangle$, ign	3%
$(\tau_E)_{\text{emp}}$ (s)	0.45
$t_{\text{pulse}} / (\tau_e)_{\text{emp}}$	> 40
Fusion power (alphas & neutrons) (MW)	80
Max Neutron wall loading (MW/m^2)	~ 3.2
Max heat loading of vacuum wall (MW/m^2)	~ 0.8

Table II
Parameters of EF System

Coil Major Radii

R_1 (m)	1.2
R_2 (m)	2.2
R_3 (m)	4.2

Coil current	Initial	Final
I_1 (MA)	1.8	2.8
I_2 (MA)	0.4	0.6
I_3 (MA)	0.7	1.2

$$n = - \frac{R}{B_v} \frac{dB_v}{dR} \quad 1.3$$

Initial energy (MJ) 15

Final energy (MJ) 35

Increase in energy during compression (MJ) 20

τ_{comp} (s) ≤ 0.1

Peak Power (MW) ≤ 200

Power Supply Inductive Storage

Table III

TF Magnet

Dimensions

Height (m)	2.5
Outer Radius, R_{out} (m)	3.4
Inner Radius, r_{ohm} (m)	0.35
Major Radius of center of magnet bore (m)	1.95
B_T at Major Radius of center of magnet bore (T)	8.1
Field at final plasma (T)	12.5
Peak field (T)	20.5
Total TF current (A)	8×10^7
Stored energy (J)	8.9×10^8
Stresses (Pa)	
Circumferential	8×10^7
Vertical tensile at inboard trunk	3.6×10^8
Bending stresses, max	3.0×10^8
Resistive power (at 77°K)	60 MW
Resistive power (after 20s flat top)	200 MW
Energy dissipation per 20s pulse	
Electrical	1.2 GJ
Nuclear (20s ignited operation)	1.3 GJ
Peak magnet temperature, flat top	300 °K
Weight (m tons)	530
Liquid nitrogen evaporation per 20 s pulse (ℓ)	8000

Table IV

OH Magnet

Dimension

Outer diameter (m)	0.6
Inner Diameter (m)	0.36
Height (m)	2.5
Weight (m ton)	4

Initial plasma (V·s)

Resistive Volt-seconds	~ 4.0
Inductive Volt-seconds	7.5
EF contribution	8.9
OH contribution	2.6

Final plasma (V·s)

Inductive volt-seconds	6.2
EF contribution	7.25
OH contribution	3.0
Change of OH during compression	0.4
Peak stress in OH magnet (Pa)	7×10^7
Dissipation at peak field (MW)	3

Table V
Lifetime Expectancy of Insulation [†]

Organic

Polyester (burn-s)	500
Reinforced Epoxy (burn-s)	5,000
Reinforced Polyimide (burn-s)	5,000

Inorganic

Mica (burn-s)	500,000
Alumina (burn-s)	500,000

[†] Radiation limits taken from R.D. Hay and E.J. Rapperport,
"Review of Electrical Insulators in Superconducting Magnets
for Fusion Research," M.E.A. Report, Cambridge, MA, (April 1976).

Table VI
Neutral Beam System

Injection	near perpendicular
P_B (MS = 1) (MW)	12.5
Wb (MS = 1) (keV)	120
Neutral beam lines	6
Beam access (m^2)	1.2
Beam energy density (kw/cm^2)	1.
Beam on time (s)	~ 0.6
Travel distance in high magnetic field from end of neutralizer to plasma chamber	$\leq 0.6m$

Table VII
Ripple Cancelling Coils

Shape	Rectangular
Dimensions	
height (m)	0.7
width (m)	0.6
Position	
mean radius	3.75
displacement with respect to beam center line	± 0.65
Current (A)	$\sim 2 \times 10^6$
Magnetic energy per port (MJ)	~ 7
Tensile Stresses (Pa)	$< 1.10^8$
Current density in coil A/m ²	$\sim 5 \times 10^7$
Energized time	$\sim 5s$

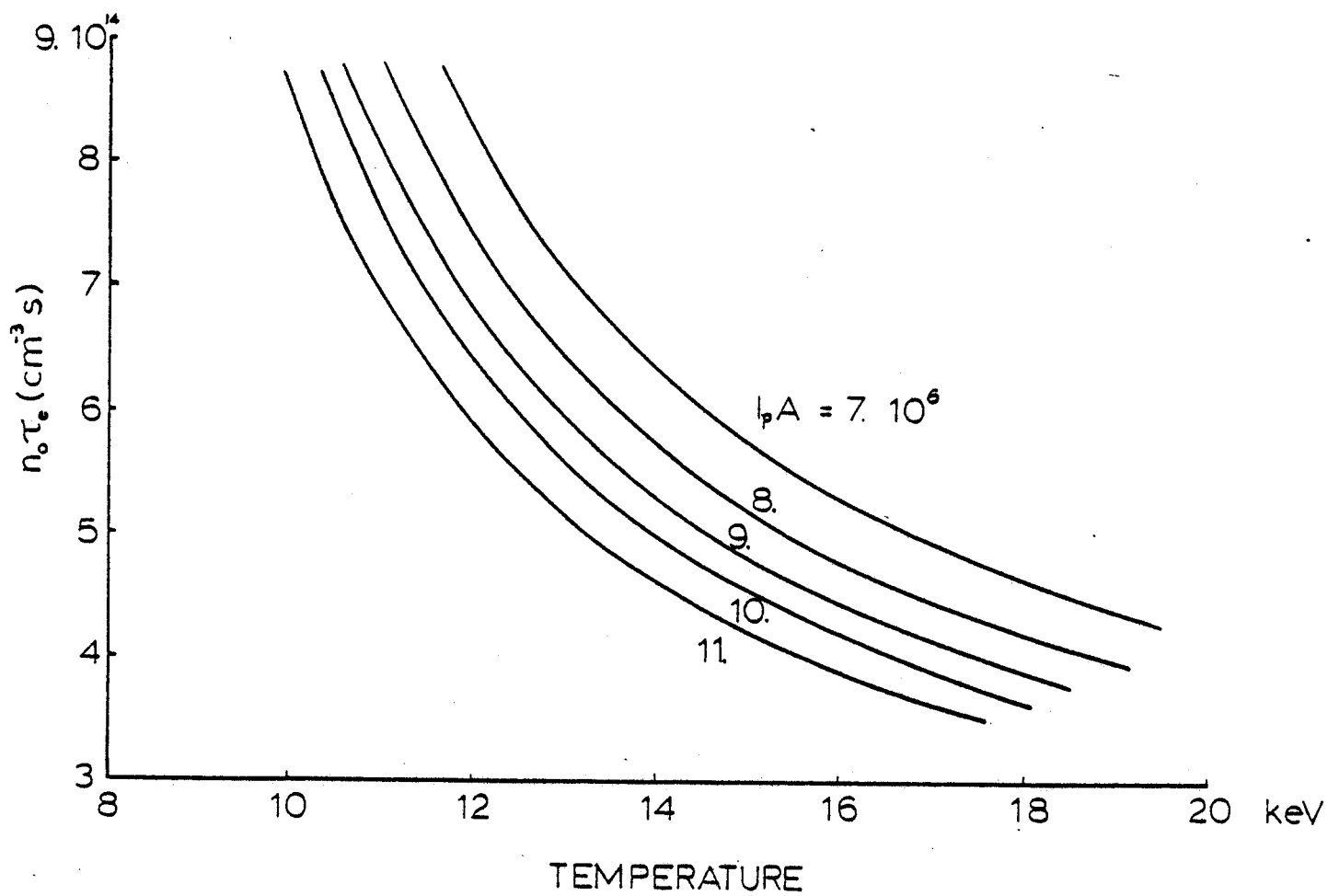


Figure 1

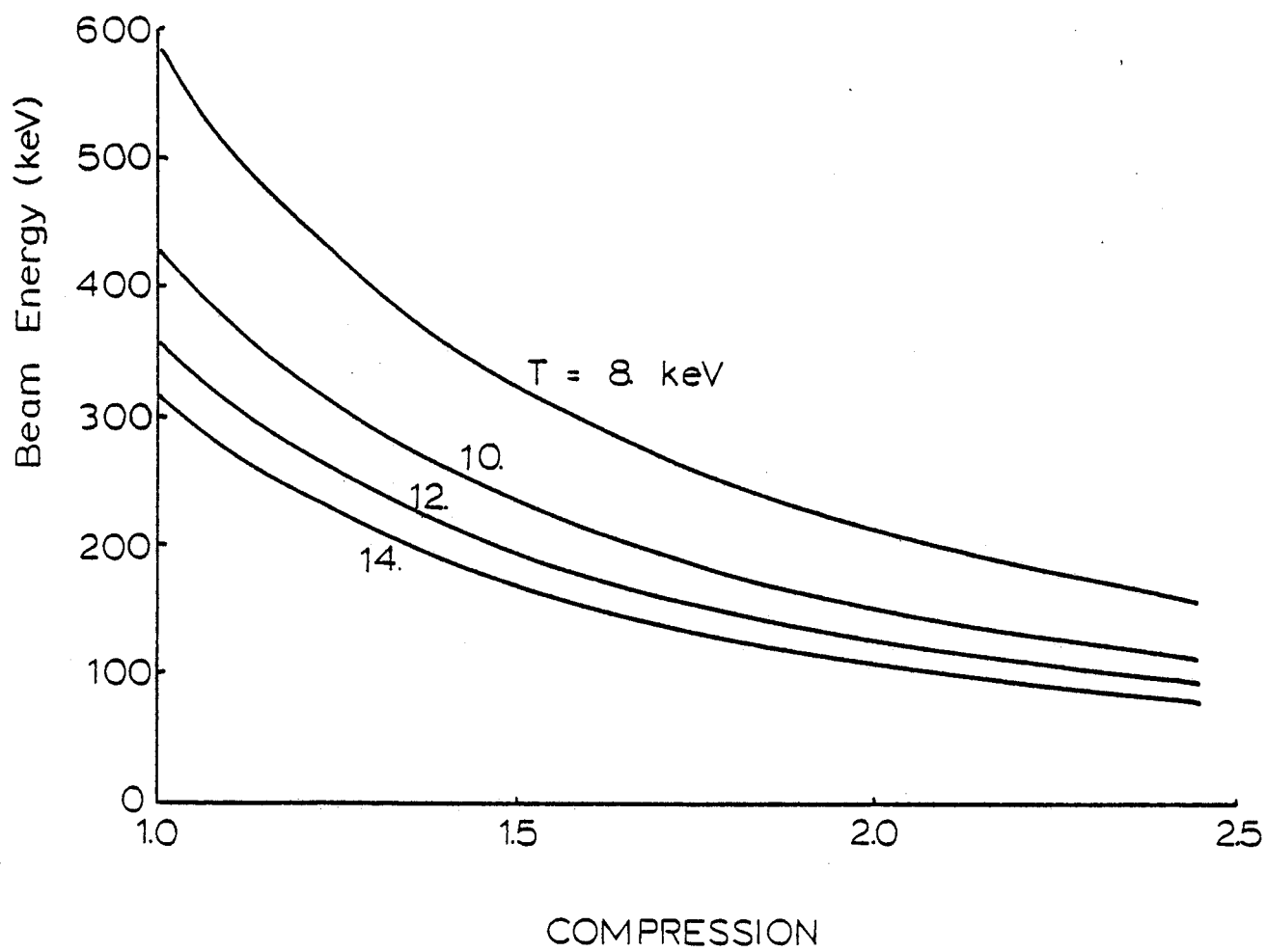


Figure 2

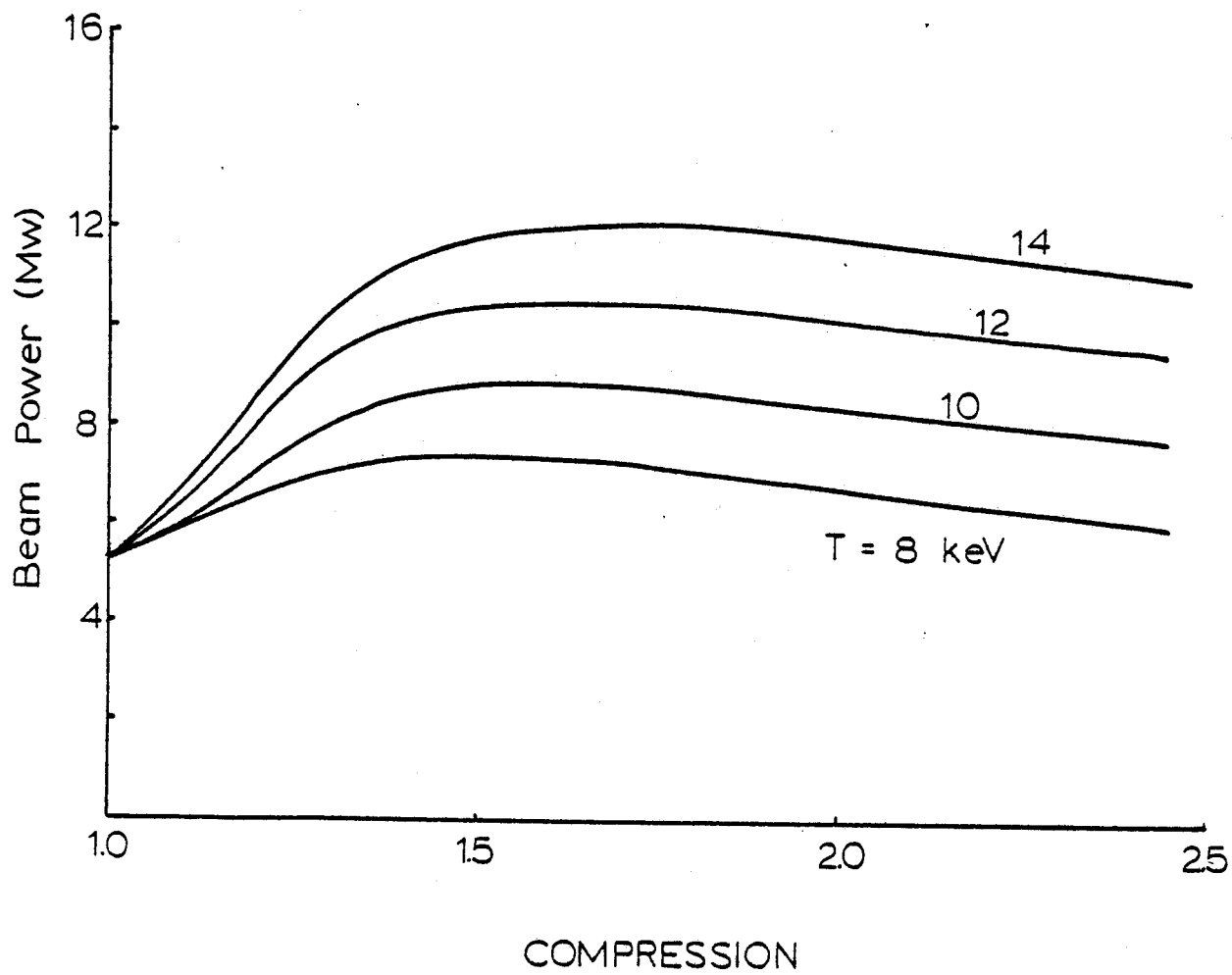


Figure 3

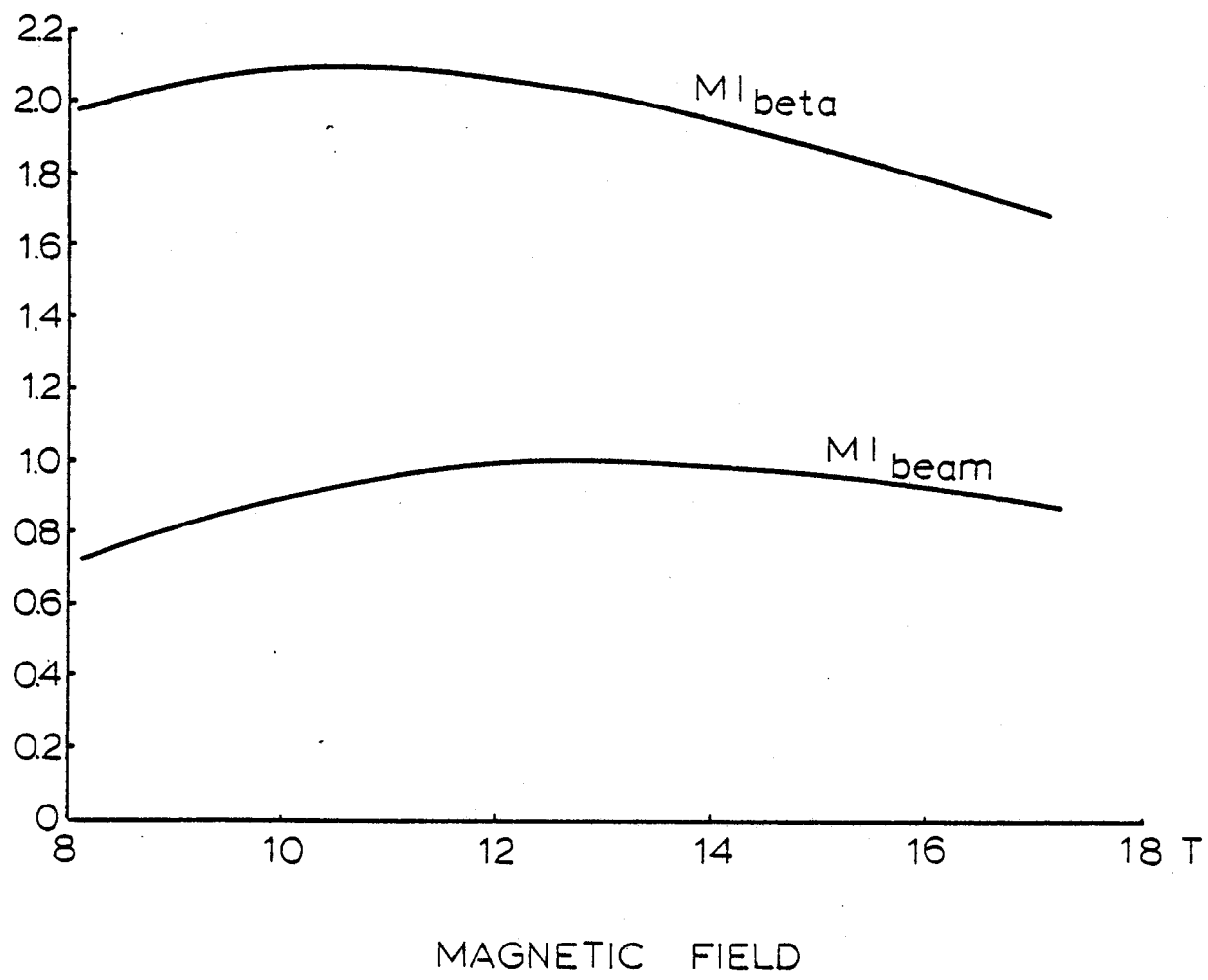


Figure 4

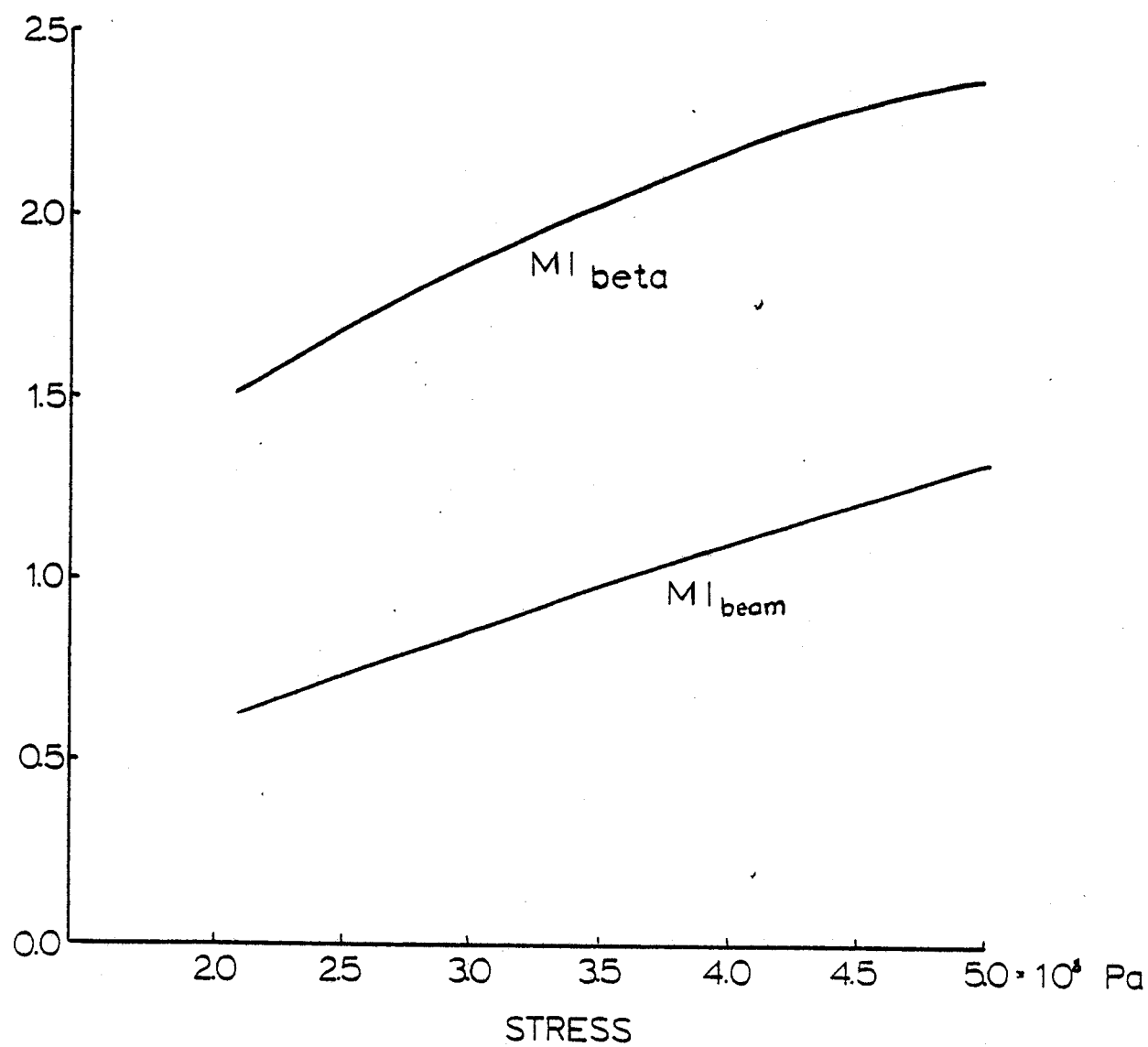


Figure 5

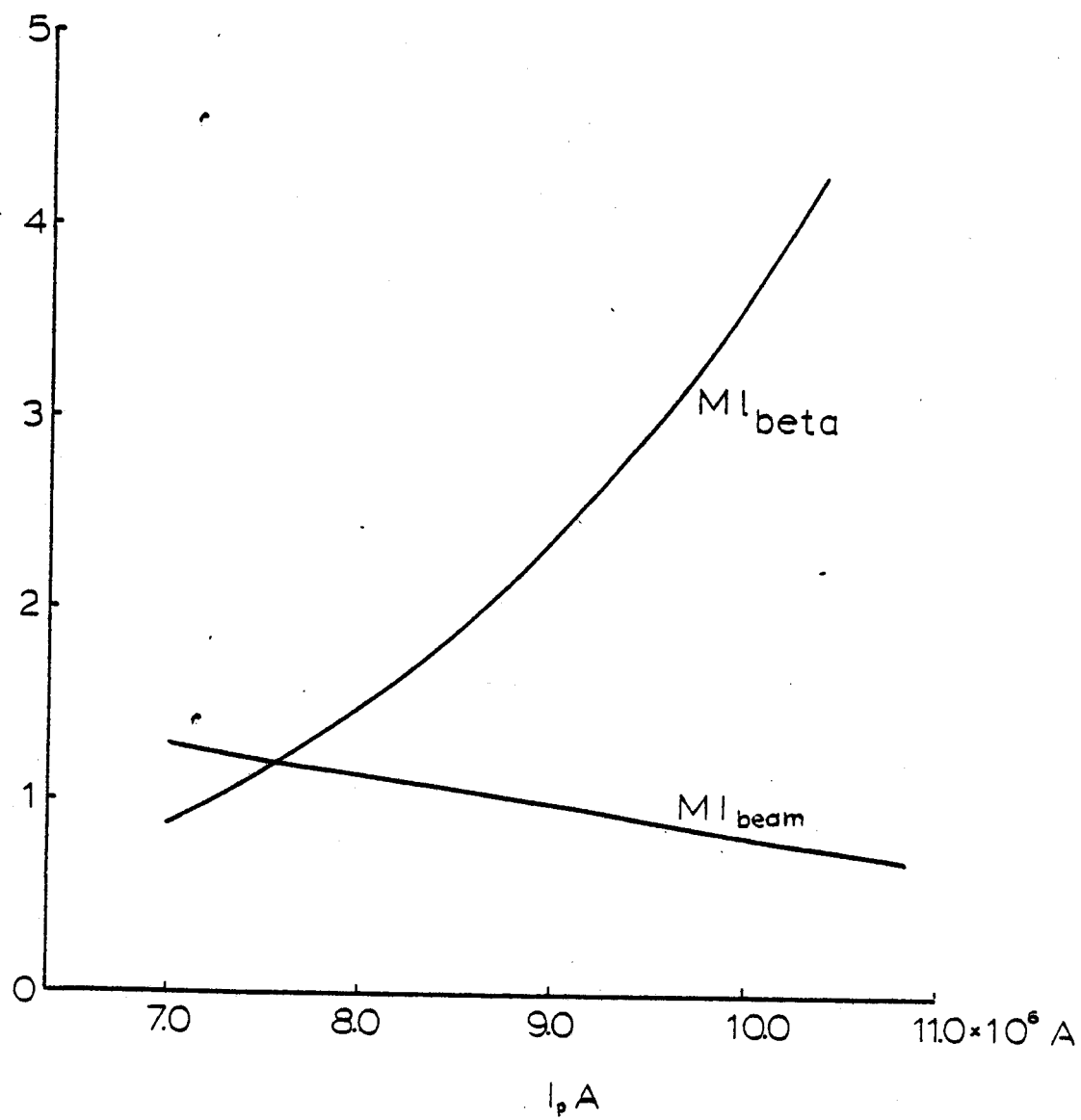


Figure 6

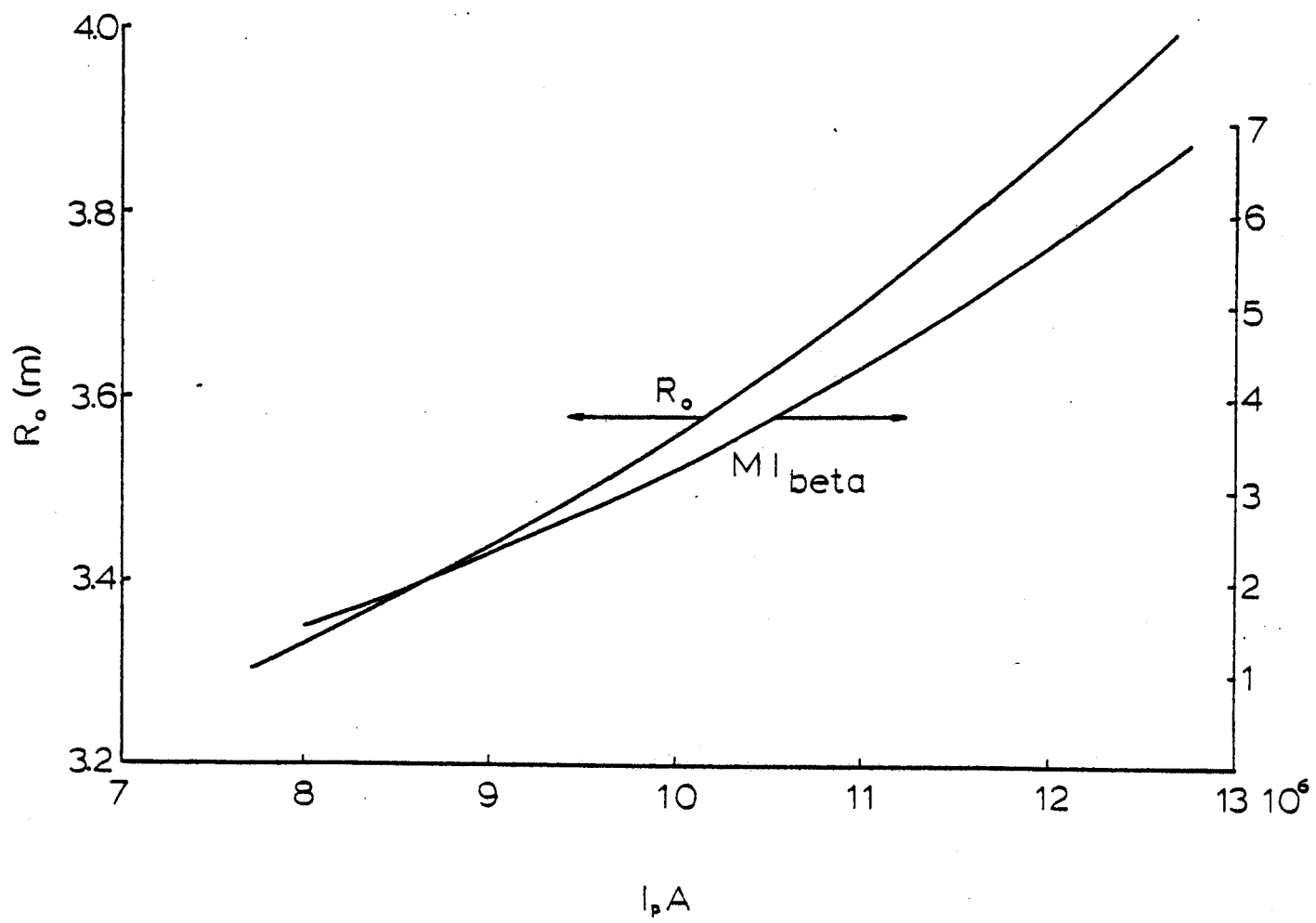


Figure 7

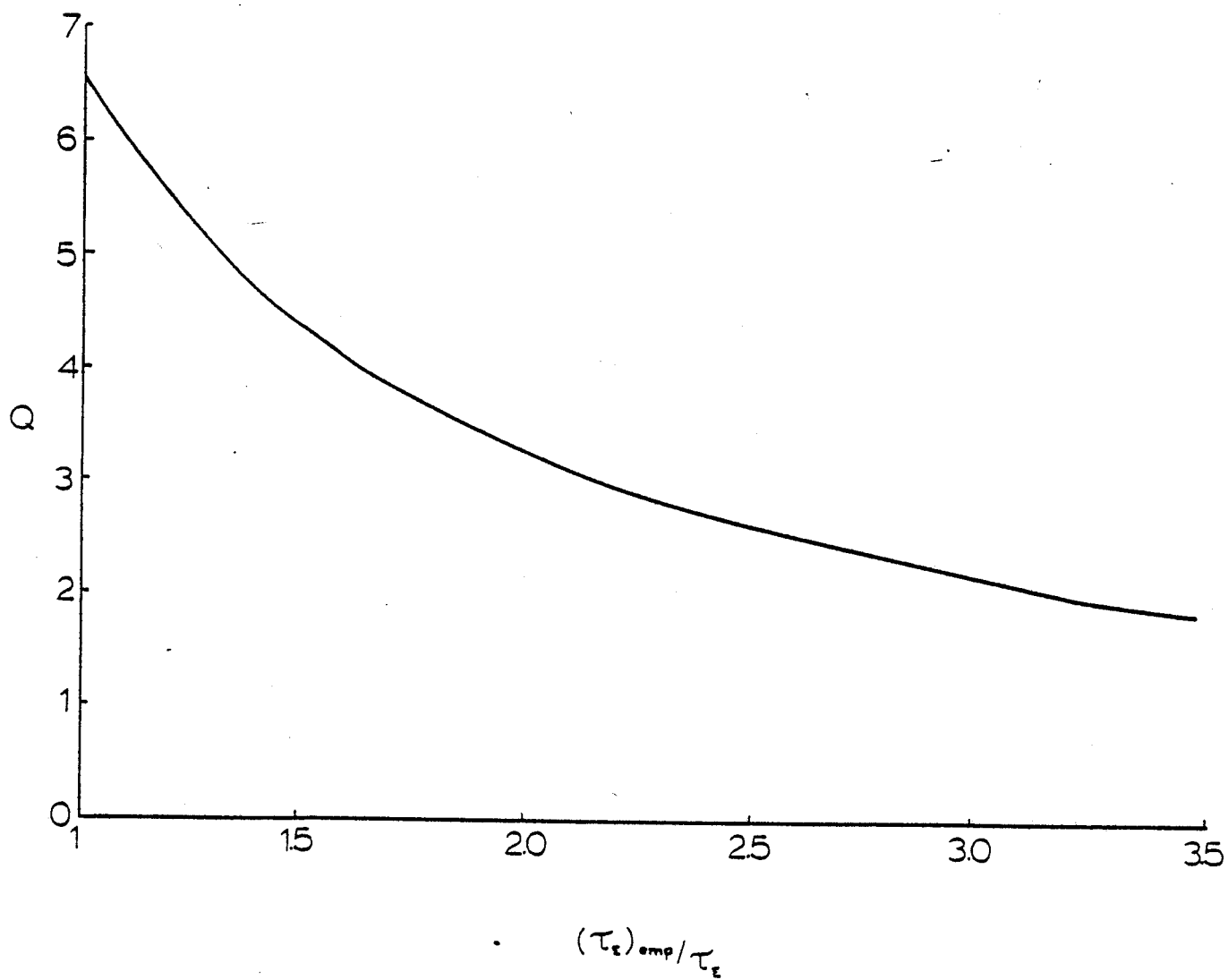


Figure 8

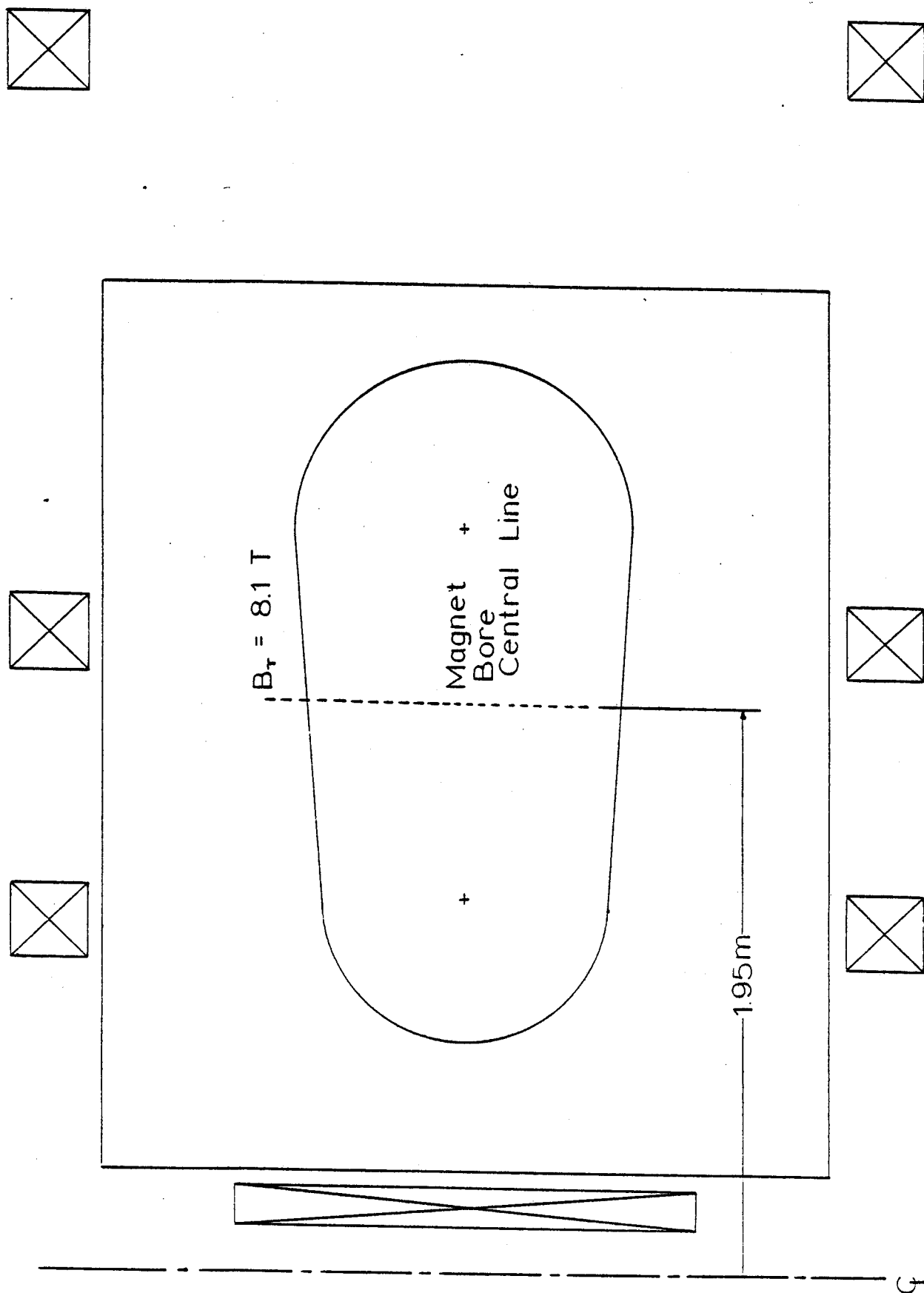


Figure 9

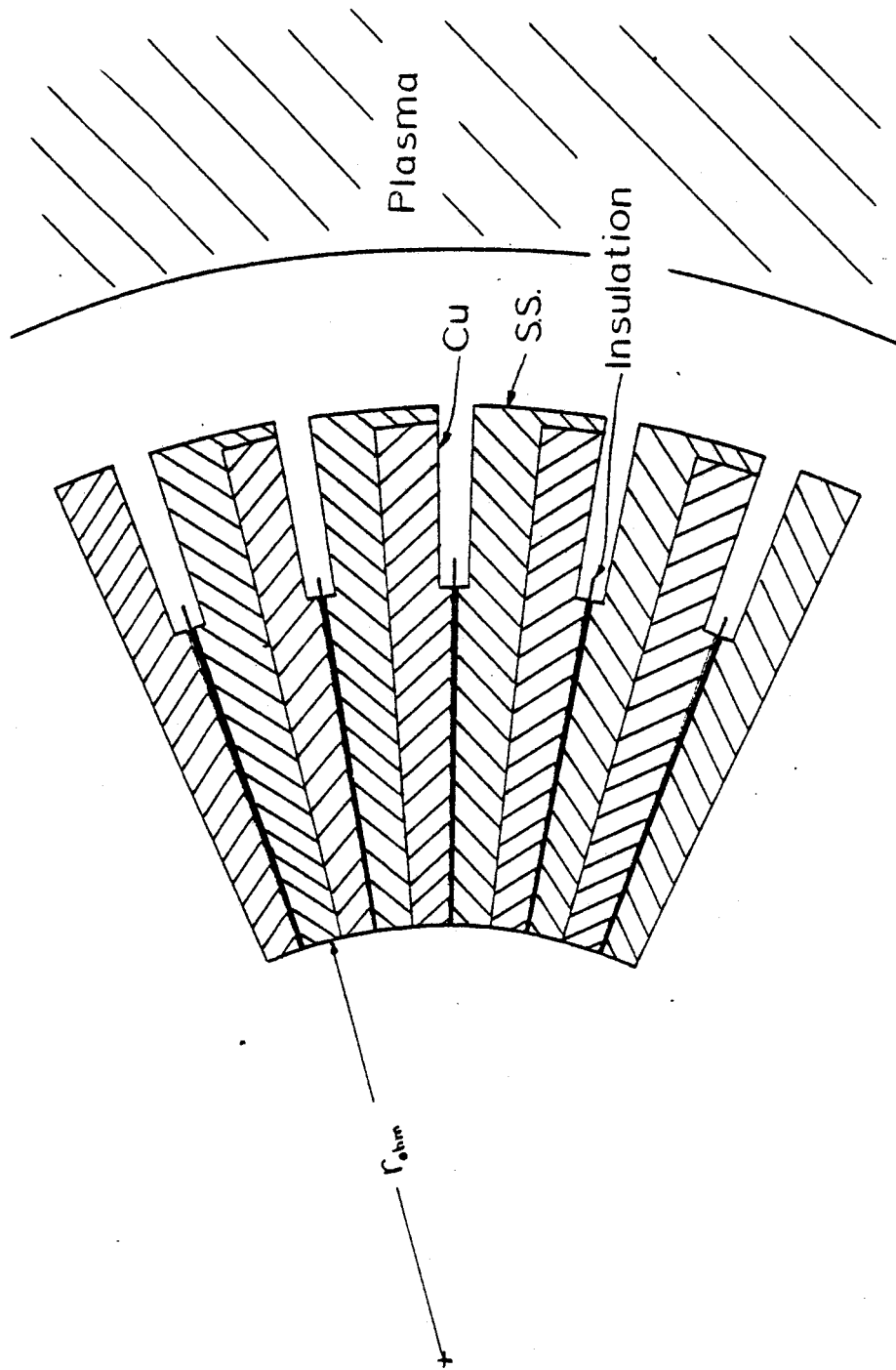


Figure 10

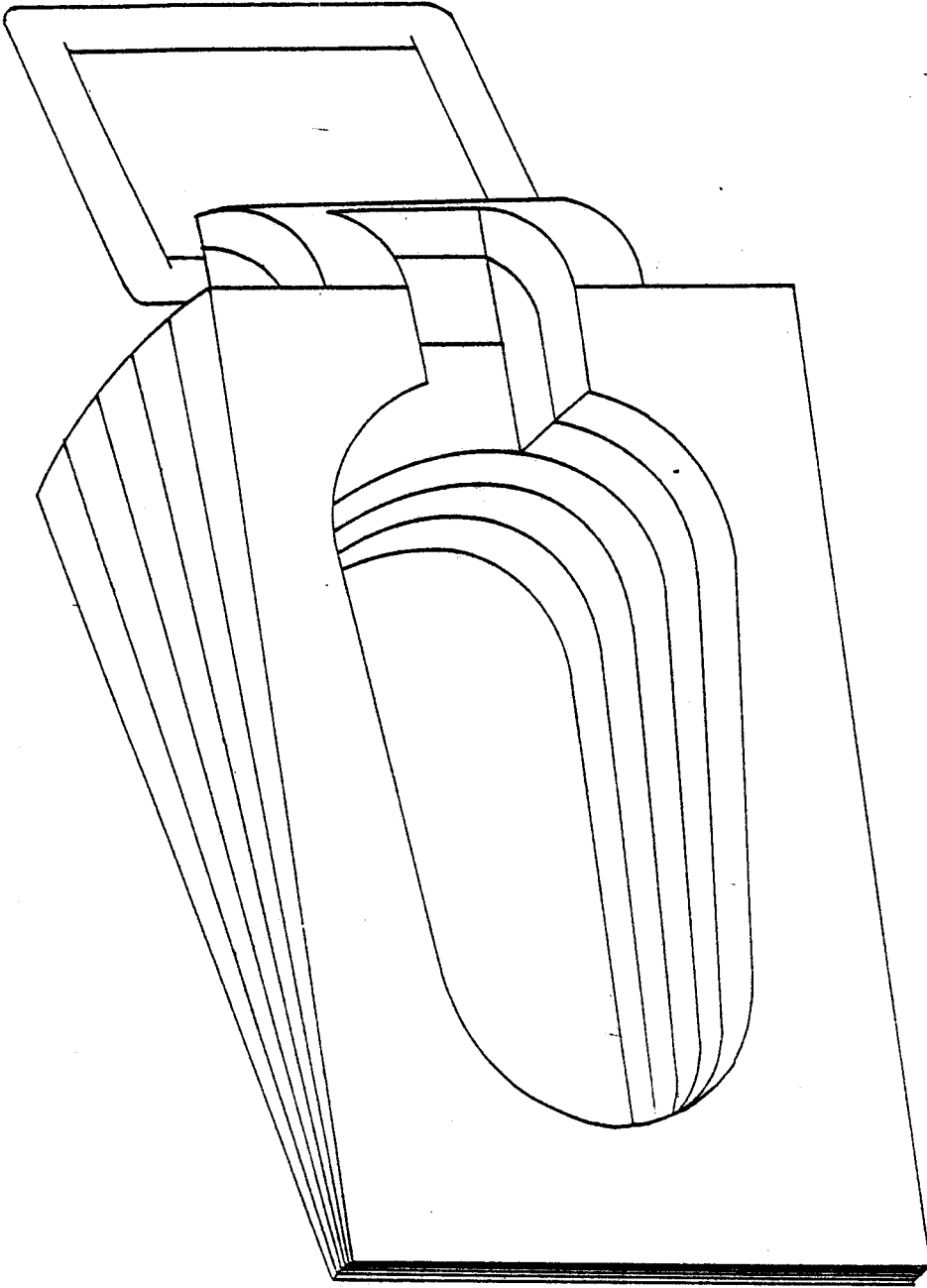


Figure 11

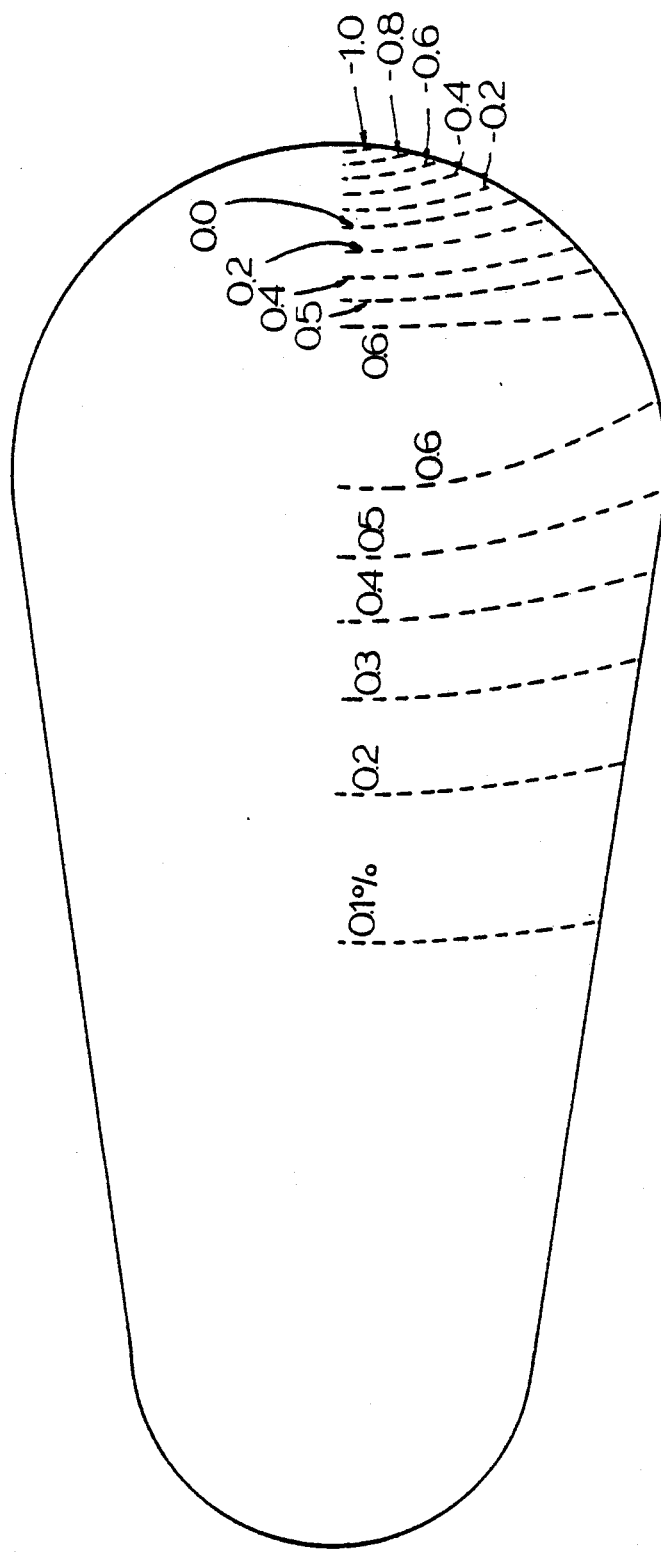


Figure 12